Spectral Sensitization of Large-band-gap Semiconductors (Thin Films and Ceramics) by a Carboxylated Bis(1,10-Phenanthroline)copper(I) Complex*

Nicolás Alonso-Vante,[a] Jean-François Nierengarten[b] and Jean-Pierre Sauvage[b]
[a] *Hahn-Meitner-Institut, Abt. Solare Energetik, Glienicker Strasse 100, D-14109 Berlin, Germany*
[b] *Laboratoire de Chimie Organo-Minérale, Université Louis Pasteur, 1, rue Blaise Pascal, F-67008 Strasbourg Cedex, France*

Photoelectrochemical cells based on colloidal films of titanium dioxide and zinc oxide ceramic electrodes sensitized by a bis(2,9-diphenyl-1,10-phenanthroline)copper(I) complex modified at the *para* positions with NaO_2C groups, were investigated in an aqueous medium using hydroquinone as electron donor. The sensitizing effect is greater with the films due to the enhanced geometric area projection. The photocurrent-action spectrum obtained with this complex covers almost the whole of the solar visible region. The quantum efficiency was found to depend on the degree of surface coverage by the complex. In a solar-cell arrangement the open-circuit photovoltage was 0.6 V with a small short-circuit photocurrent of *ca.* 0.6 mA cm^{-2} in iodide-containing propylene carbonate.

In (photo)electrochemistry the modification of electrode surfaces represents a valuable strategy for tailoring interesting reactions mediated by the adduct deposited on the surfaces.[1,2]

To take advantage of the visible solar spectrum, sensitization of large-band-gap semiconductors (known for their relatively higher stability to corrosion in aqueous media in comparison to small-band-gap semiconductors) *via* organic dyes was popular in the past[3-7] and is still under investigation.[8-10] There is renewed interest in sensitization *via* ruthenium-based transition-metal complexes[11] since the work of Grätzel and collaborators.[12-14] Their approach of collecting light by the scattering process while maintaining efficient carrier injection, was based on the use of highly porous, *i.e.*, large surface area, titanium dioxide anatase substrates.

The photochemical and spectroscopic properties of some $[CuL_2]^+$ complexes with differently substituted inter-penetrating ligands, *e.g.* L = 2,9-diphenyl-1,10-phenanthroline has been reported.[15,16] The sensitization effect of copper(I) complexes with various phenylated phenanthrolines (insoluble in water) was observed previously in photoelectrochemical cells based on semiconducting zinc oxide ceramic electrodes.[17] The aim of the present work was to explore the sensitizing effect of a copper(I) complex with phenanthroline ligands bearing CO_2^- terminal groups on large-band-gap semiconducting oxide electrodes such as colloidal TiO_2 and ceramic ZnO.

Experimental

Synthesis.—General. The compounds $[Cu(MeCN)_4]BF_4$ and *p*-bromobenzyl tetrahydropyran-2-yl ether **I** were prepared as reported.[18,19] All other chemicals were of the best commercially available grade used without further purification. Proton NMR spectra were recorded with a Bruker WP200SY spectrometer, mass spectra on a Thomson T.H.N. 208 (chemical ionization, CI) spectrometer. Melting points (uncorrected) were measured with a Büchi SMP20 apparatus. Infrared spectra were recorded on a Perkin-Elmer 457 spectrophotometer in potassium bromide discs.

2-[(p-*Tetrahydropyranyloxymethyl*)*phenyl*]-1,10-*phenanthroline* **III**. A 1.57 mol dm^{-3} *n*-butyllithium solution (22.0 mmol, 14.0 cm^3) was added by syringe at room temperature to an argon-flushed, stirred, degassed solution of *p*-bromobenzyl tetrahydropyran-2-yl ether (6.0 g, 22.15 mmol) in dry diethyl ether (100 cm^3). The corresponding *p*-lithio compound **II** precipitated as a beige solid. After the mixture had been stirred for 1 h under argon at room temperature a sensitive qualitative colour test[20] indicated the completion of the lithiation. Using the double-ended needle-transfer technique, the mixture was added under argon to a degassed suspension of commercial 1,10-phenanthroline (3.24 g, 18.0 mmol) in dry ether (200 cm^3) cooled to 0 °C (ice–water bath). The resulting dark red mixture was stirred for 4 h under argon at 0–4 °C then hydrolysed with water. The bright yellow ether layer was decanted and the aqueous layer extracted three times with 100 cm^3 portions of CH_2Cl_2. The combined organic layers were thereafter rearomatized by successive additions ($\approx$ 10 g) of MnO_2 (Merck) with magnetic stirring. This reoxidation, easily followed by TLC and the disapperance of the yellow colour, was ended after the addition of 60 g MnO_2. The mixture was dried over $MgSO_4$, the black slurry filtered on sintered glass and the filtrate evaporated to dryness to give the crude product. Column chromatography on silica gel (CH_2Cl_2–2% MeOH) indicated a 68% yield (4.56 g, 12.3 mmol). ^1H NMR($CDCl_3$) of the pale yellow glassy product: δ 9.27 (dd, 1 H, H^9, ^3J = 4.4, ^4J = 1.7), 8.35 (d, 2 H, H_o, ^3J = 8.3), 8.32 (d, 1 H, H^4, ^3J = 8.4), 8.29 (dd, 1 H, H^7, ^3J = 8.1, ^4J = 1.7), 8.12 (d, 1 H, H^3, ^3J = 8.4), 7.81 (AB, 2 H, $H^{5,6}$, ^3J = 8.8), 7.66 (dd, 1 H, H^8, ^3J = 8.1, $^3J'$ = 4.4), 7.55 (d, 2 H, H_m, ^3J = 8.3), 4.76 (AB, 2 H, aryl CH_2O, ^2J = 12.4 Hz), 4.74 (m, 1 H, H^2 of pyranyl), 3.76 (m, 2 H, H^6 of pyranyl) and 1.9–1.5 (m, 6 H, H^{3-5} of pyranyl).

2,9-*Bis*[(p-*tetrahydropyranyloxymethyl*)*phenyl*]-1,10-*phenanthroline* **IV**. The organolithium compound **II** was prepared as described above by treatment of the bromide **I** (2.0 g, 7.4 mmol) with 0.99 equivalent of $LiBu^n$. Using the double-ended needle-transfer technique, the resulting mixture was added under argon to a degassed suspension of compound **III** (1.40 g, 3.78 mmol) in dry ether (80 cm^3) cooled to 0 °C (ice–water bath). The dark red mixture was stirred for 3 h under argon at 0–5 °C, then hydrolysed with water. The bright yellow ether layer was decanted and the aqueous layer extracted three times with 100 cm^3 portions of CH_2Cl_2. The combined organic

* *Non-SI unit employed:* eV $\approx$ 1.60 × 10^{-19} J.

layers were rearomatized by addition of MnO_2 (50 g). The mixture was dried over $MgSO_4$, the black slurry filtered on sintered glass and the filtrate evaporated to dryness to give crude compound **IV**. Column chromatography on silica gel (CH_2Cl_2–1.5% MeOH) showed a 79% yield (1.68 g, 3.0 mmol). ^1H NMR ($CDCl_3$) of the pale yellow glassy product: δ 8.45 (d, 4 H, H_o, ^3J = 8.2), 8.34 (d, 2 H, H^{4-7}, ^3J = 8.4), 8.16 (d, 2 H, H^{3-8}, ^3J = 8.4), 7.81 (s, 2 H, $H^{5,6}$), 7.60 (d, 4 H, H_m, ^3J = 8.2), 4.78 (AB, 2 H, aryl CH_2O, ^2J = 12.4 Hz), 4.77 (m, 2 H, H^2 of pyranyl), 3.80 (m, 4 H, H^6 of pyranyl) and 2.0–1.5 (m, 12 H, H^{3-5} of pyranyl) (Found: C, 76.6; H, 6.7; N, 4.6. Calc. for $C_{36}H_{36}N_2O_4 \cdot 0.33H_2O$: C, 76.3; H, 6.5; N, 4.9%).

2,9-*Bis*[(p-*hydroxymethyl*)*phenyl*]-1,10-*phenanthroline* **V**. To a refluxing solution of compound **IV** (2.47 g, 4.4 mmol) in dry ethanol (500 cm^3) was added dropwise during 45 min a solution of toluene-*p*-sulfonic acid (2.10 g, 11.05 mmol) in dry ethanol (50 cm^3). Heating was continued for 4 h. The volume was then reduced to 10 cm^3 and addition of water (300 cm^3) precipitated the crude product. After neutralization with a dilute NaOH solution, the beige solid was filtered off, air dried and finally dried under high vacuum in the presence of P_2O_5 to yield pure compound **V** as a beige powder in 90% yield (1.56 g, 4.0 mmol), m.p. 234–236 °C. ^1H NMR [$(CD_3)_2CO$]: δ 8.59 (d, 4 H, H_o, ^3J = 8.4), 8.51 (d, 2 H, H^{4-7}, ^3J = 8.5), 8.36 (d, 2 H, H^{3-8}, ^3J = 8.5), 7.95 (s, 2 H, $H^{5,6}$), 7.61 (d, 4 H, H_m, ^3J = 8.4) and 4.77 (d, 4 H, CH_2, ^4J = 5.8 Hz) (Found: C, 77.5; H, 5.4; N, 6.7. Calc. for $C_{26}H_{20}N_2O_2 \cdot 0.5H_2O$: C, 77.8; H, 5.3; N, 7.0%).

2,9-*Bis*(p-*formylphenyl*)-1,10-*phenanthroline* **VI**. Manganese dioxide (14 g, 0.16 mmol) was added with efficient stirring to an argon-purged solution of compound **V** (400 mg, 1.02 mmol) in acetone (350 cm^3). The mixture was stirred for 1 h under argon at room temperature, then $MgSO_4$ was added to ease the removal of the MnO_2 by filtration. The mixture was filtered, washed with CH_2Cl_2 and the filtrate evaporated to dryness to yield pure compound **VI** in 87% yield (344 mg, 0.89 mmol). This compound was obtained as a secondary product in a previously published reaction and was fully characterized.[21]

2,9-*Bis*(p-*carboxyphenyl*)-1,10-*phenanthroline* **VII**. To a magnetically stirred suspension of compound **VI** (500 mg, 1.29 mmol) (it dissolves partially) in acetone (350 cm^3) kept at 50–55 °C was added dropwise over 30 min a solution consisting of Jones reagent (5 cm^3)[22] and acetone (50 cm^3). Heating was continued for 5 h. After cooling, isopropyl alcohol was added dropwise to destroy the excess of Jones reagent. The solvent was removed and the crude deep green solid washed with water until disappearance of the green colour. The crude dicarboxylic acid **VII** was partially dissolved in a dilute NaOH solution and precipitated by addition of dilute hydrochloric acid. The yellow solid was filtered off, washed with water, air dried and finally dried under high vacuum in the presence of P_2O_5 to yield the pure compound in its chlorhydrate form (**VII**·HCl) as a yellow powder in 86% yield (506 mg, 1.11 mmol), m.p. > 280 °C. IR(KBr): 3076, 2564 and 1682 cm^{-1}. ^1H NMR [$(CD_3)_2SO$]: δ 8.68 (d, 4 H, H_o, ^3J = 8.4), 8.66 (d, 2 H, H^{4-7}, ^3J = 8.5), 8.52 (d, 2 H, H^{3-8}, ^3J = 8.5), 8.21 (d, 4 H, H_m, ^3J = 8.4 Hz) and 8.07 (s, 2 H, $H^{5,6}$) (Found: C, 67.9; H, 4.1; N, 6.0. Calc. for $C_{26}H_{16}N_2O_4 \cdot HCl$: C, 68.3; H, 3.8; N, 6.1%). Mass spectrum (CI): *m/z* 419 (*M* − H) and 375 (*M* − CO_2H).

Complex **1**. Compound **VII** (250 mg, 0.548 mmol) was dissolved in an aqueous 1 mol dm^{-3} NaOH solution (100 cm^3). After stirring for 3 h, the sodium salt was precipitated by addition of NaCl until saturation. It was filtered off, rapidly washed with cold water, air dried and finally dried under high vacuum in the presence of P_2O_5 to give a pale yellow powder (230 mg, 0.496 mmol; 90%). Using the double-ended needle-transfer technique, $[Cu(MeCN)_4]BF_4$ (78 mg, 0.248 mmol) in degassed MeCN (40 cm^3) was added under argon at room temperature to a stirred degassed solution of the pale yellow powder (230 mg) in methanol (100 cm^3). The mixture turned dark red instantaneously, indicating the formation of complex **1**. After stirring the solution for 4 h at room temperature the solvents were evaporated to dryness. The dark red residue was recrystallized from CH_2Cl_2–methanol–water to give dark red needles of pure complex **1** as its BF_4^- salt in 60% yield (160 mg, 0.148 mmol), m.p. > 280 °C. IR(KBr): 1590 cm^{-1}. ^1H NMR (CD_3OD): δ 8.59 (d, 4 H, H^{4-7}, ^3J = 8.4), 8.00 (s, 4 H, $H^{5,6}$), 7.96 (d, 4 H, H^{3-8}, ^3J = 8.4), 7.46 (d, 8 H, H_o, ^3J = 8.2) and 7.17 (d, 8 H, H_m, ^3J = 8.2 Hz) (Found: C, 47.1; H, 4.2; N, 4.5. Calc. for $C_{52}H_{28}BCuF_4N_4Na_4O_8 \cdot 14H_2O$: C, 46.9; H, 4.2; N, 4.2%).

Electrode. Anatase films were produced from a viscous colloidal solution prepared from titanium dioxide aggregates (P25 Degussa) as described.[12,14] Anatase thin films were obtained by spin coating (at 2000 revolutions min^{-1}) 5–10 μl cm^{-2} on conducting glass substrates (fluorine-doped tin dioxide layers) with one edge masked with Scotch tape for electrical contact. This procedure resulted in homogeneity of the films which had a thickness which varied between 1 and 2 μm according to the content of TiO_2 in the colloidal solution. These films were subsequently fired at 450 °C for 30 min. The ceramics were prepared from commercial high-grade zinc oxide powder (Merck) by sintering as described.[23] The ohmic contact was made on the back of the samples with silver epoxy paste (Elecolit). Both systems were mounted on copper wire. An epoxy resin (no. 10, XR-5241, 3M, Scotchcast) was employed to encapsulate all metallic parts of the electrode. The zinc oxide ceramic surface was etched with 6 mol dm^{-3} HCl in solution for 30 s.

Photoelectrochemical Measurements.—A standard electrochemical (EG&G model 273A) computer-based set-up was used for current and potential measurements. Illumination was provided by a tungsten–halogen lamp (250 W). A 500 nm band-pass filter (K-50 Balsers) was used in all experiments unless otherwise noted. The Pyrex cell consisted of a single compartment having a three-electrode configuration. Platinum and Hg–Hg_2SO_4, 0.5 mol dm^{-3} H_2SO_4 [0.65 V *vs.* normal hydrogen electrode (NHE)] were used as counter and reference electrodes, respectively. Photocurrent-action spectra were recorded with a monochromator (Kratos GM). For the quantum yield determination, the monochromatic light intensity was measured with a silicon diode (Siemens) placed in the photoelectrochemical cell. The photoelectrode was polarized with a Pine potentiostat. The base electrolyte employed containing hydroquinone was 0.4 mol dm^{-3} Na_2SO_4 (reagent grade; Merck), pH 6.5.

Results and Discussion

Absorption and Redox Properties.—The visible absorption spectrum of a methanolic solution of complex **1** (measured with an Omega 10 spectrometer) is shown in Fig. 1(*a*). Several absorption bands (metal-to-ligand charge transfer, m.l.c.t.) are present in the visible range, the maximum being located at 440 nm. If stabilized at the semiconducting surface, the broad range of visible light absorption renders this compound an attractive sensitizer. The absorption coefficient at the maximum is 3000 dm^3 mol^{-1} cm^{-1}. The emission line has its maximum at 680 nm

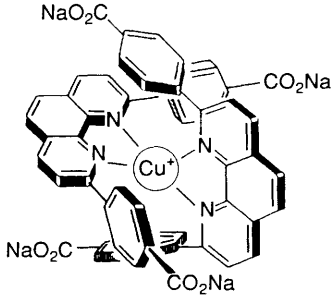

1

(298 K). Similar values were obtained with the corresponding non-carboxylated copper(I) complex.[24] This allows us to derive that the 0–0 transition energy has a value of *ca.* 2 eV. The absorption coefficient of the present complex is a factor of *ca.* 3.7 and 4.7 lower than, *e.g.*, that of $[Ru^{II}(bipy)_2(L')]^{2+}$ [bipy = 2,2'-bipyridine, L' = 4,4'-bis(nonadecyl)-2,2'-bipyridine] (refs. 23 and 25) and $[Ru^{II}L_2(SCN)_2]\cdot 2H_2O$ (L = 2,2'-bipyridine-4,4'-dicarboxylic acid),[14] respectively. This apparent disadvantage *vis-à-vis* the low photon absorption might be surmounted by increasing the copper(I) complex concentration.

The redox properties were studied by cyclic voltammetry with a platinum (or glassy carbon) electrode *vs.* an aqueous mercury sulfate reference electrode (0.64 V *vs.* NHE) in acetonitrile solutions containing 0.1 mol dm^{-3} $[NBu_4][ClO_4]$. The redox potentials were corrected by subtracting the junction-potential contribution (ε_j = 0.09 V). For the non-carboxylated complex (soluble in this medium) a redox potential of 0.45 V *vs.* NHE was determined. Owing to the insolubility of the carboxylated complex in acetonitrile, a drop of this complex, dissolved in methanol solution, was placed on the platinum (or glassy carbon) surface and air-dried. The value of the redox potential measured was 0.91 V *vs.* NHE. The difference of 0.46 V between the carboxylated and the unsubstituted analogue might be attributed to the electron-withdrawing properties of the CO_2^- attached to the phenyl groups.

Kubelka–Munk values, *i.e.*, the ratio of the absorption and scattering, K–M = $(1 - R)^2/2R$, deduced from reflectance (R) measurements in an integrating sphere on coated titanium dioxide layers left overnight in two different concentrations of complex **1** are depicted in Fig. 1(*b*), normalized to an uncoated titanium dioxide film. As can be seen, similar features for **1** in the adsorbed state compared to a solution in methanol are obtained [Fig. 1(*a*)]. The intensity of the absorption in the adsorbed state apparently depends on the concentration of the initial solution. This observation should be regarded with caution since we cannot rigorously control the rugosity factor of the semiconducting anatase layers. A point of reference supporting this observation is that the photogenerated sensitized current, for similar semiconducting layers, increases with increasing concentration of the carboxylated complex in which the layers are dipped.

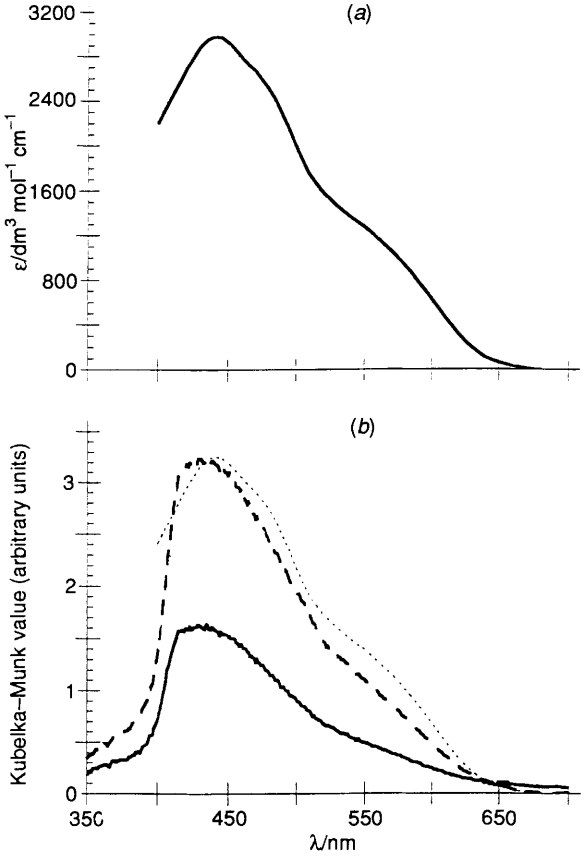

Fig. 1 (*a*) Absorption spectrum of a 5 × 10^{-3} mol dm^{-3} solution of the copper(I) complex **1** in methanol. (*b*) Kubelka–Munk spectra deduced from reflectance spectra in an integrating sphere on titanium dioxide films in 1 × 10^{-3} (——) and 1 × 10^{-2} mol dm^{-3} (— — —) solutions of the copper(I) complex in methanol. Spectrum (*a*) is included in (*b*) (short dashes) for comparison

Photocurrent-action Spectra on Titanium Dioxide (Anatase) Films and Zinc Oxide Ceramics.—Titanium dioxide (anatase) films are constituted of colloidal particles (average size 15 nm)[14] densely packed by the sintering process and forming a three-dimensional array of clusters giving rise to a microporous structure. Therefore, these layers are heterogeneous, in comparison with compacted semiconductors, *e.g.* zinc oxide ceramic (grain size 20 μm). Fig. 2(*a*) contrasts the photocurrent-action spectra obtained in 0.4 mol dm^{-3} Na_2SO_4 + 5 × 10^{-3} hydroquinone (pH 6.5) for anatase film substrates coated with the copper(I) complex **1** (24 h in 5 × 10^{-3} mol dm^{-3} solution in methanol).

The electron injection (or charge-separation process) is favoured when illuminating through the glass (rear) side of the electrode. At uncoated anatase films an enhancement in the quantum efficiency in the UV region, in comparison to frontal illumination, is clearly observed. Recombination losses during the transport of electrons from the outermost layer of the

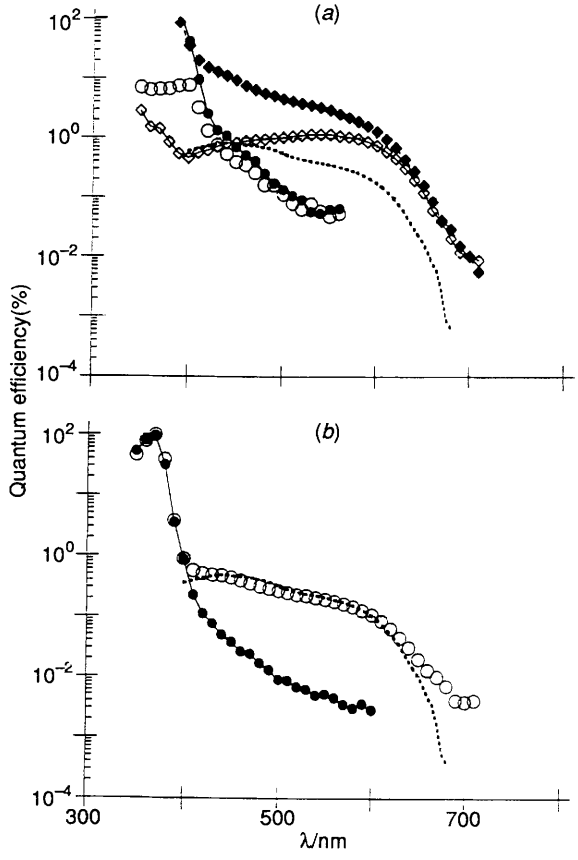

Fig. 2 Photocurrent-action spectra of (*a*) titanium dioxide films uncoated (circles) and coated (diamonds) with the copper(I) complex in 0.4 mol dm^{-3} Na_2SO_4 + 5 × 10^{-3} mol dm^{-3} hydroquinone obtained for frontal (open symbols) and rear illumination (closed symbols) respectively and (*b*) zinc oxide ceramic uncoated (●) and coated (○) with the copper(I) complex as in (*a*). The absorption spectrum measured in solution, *cf.* Fig. 1(*a*), is shown (— — —) in each case. The potential applied was 0.54 V *vs.* NHE

electrode to the rear contact can account for the lower quantum yield in frontal illumination in comparison to rear illumination. This difference might indicate that electron–hole pair separation takes place within each colloidal particle. These results are in agreement with the observations reported recently by Hagfeldt *et al.*[26] In the ultraviolet region the calculated quantum efficiency may be overestimated since the ultraviolet output of the tungsten–halogen lamp at wavelengths less than 400 nm is low (*ca.* 4%). On the other hand, the sensitizing effect of the copper(I) complex is clearly observed using either mode of illumination. In the visible region the magnitude of the quantum yield remains fairly constant. For this specific case, at 500 nm the quantum yield goes from *ca.* 1 (uncoated film) to 4% (coated film). Interestingly, the relative flatness of the photosensitized curve (frontal illumination) extends from 400 to 600 nm, in comparison to the absorption spectrum (dashed curve, scaled to the frontal illumination), and decays to a minimum value at *ca.* 700 nm. This shows that the absorption band centred at 550 nm predominates.

A steric modification of the environment of the copper(I), which is a distortion of its initial tetrahedral co-ordination, can be qualitatively explained by a different adsorption strength on active sites such as Ti^{3+} and Ti^{4+}. In this connection, *ex-situ* infrared measurements were instructive since they revealed that an absorption band at 1384 cm^{-1} for this complex in a potassium bromide matrix, attributed to C=N stretching (1300–1480 cm^{-1} deduced for bipyridine as ligand[27]), is shifted to 1398 cm^{-1} when adsorbed on titanium dioxide films. After photocurrent voltage recording in 0.4 mol dm^{-3} Na_2SO_4 + hydroquinone, this band was further shifted to 1411 cm^{-1}, remaining unchanged even after exposure of the film to air for several weeks. This shift and the relative change in intensity of the absorption band assigned to the C=O stretching mode (1592 cm^{-1}) in the adsorbed provides evidence that the interaction on the surface of TiO_2[28] is stronger than that on ZnO, see below.

In situ Raman spectroscopy and electrochemical experiments showed that the most intense characteristic Raman peak (1406 cm^{-1}) for free solid 1,10-phenanthroline shifts to 1412 cm^{-1} upon co-ordination with silver in the adsorbed state.[29] This supports the idea that the steric hindrance of the copper(I) complex is enhanced when charge is passed. Owing to the colour change in the copper(I) complex adsorbed on titanium dioxide substrates from yellowish to reddish after photoelectrochemical experiments in 0.4 mol dm^{-3} Na_2SO_4 + 5 × 10^{-3} mol dm^{-3} hydroquinone, it is expected that the photocurrent-action spectra be different in the frontal illumination mode for the TiO_2 and ZnO systems as contrasted in Figs. 2(*a*) and 2(*b*). The improvement of the quantum efficiency between 410 and 600 nm upon rear illumination is again due to a better transport of injected electrons to the rear contact.

Fig. 2(*b*) shows the photocurrent-action spectrum obtained on the zinc oxide ceramic. For comparison, the ceramic was coated using the same dipping time (analogous to the titanium dioxide film) in a similar concentrated copper(I) complex solution. The quantum yield obtained in this system is about one order of magnitude lower than that obtained in the titanium dioxide system under the same conditions. Furthermore, the photocurrent-action spectrum exhibits the same characteristic as that of the absorption spectrum of a solution of the carboxylated complex, see Fig. 2(*a*).

Photocurrent–Potential Characteristics of Sensitized Electrodes.—Typical photocharacteristics, in an aqueous medium (0.4 mol dm^{-3} Na_2SO_4 + 5 × 10^{-3} mol dm^{-3} hydroquinone), for the system described in Fig. 2(*a*) are shown in Fig. 3(*a*) (see curves 1, 1a and 1b). The illumination was provided *via* a band-pass filter (500 nm) using the modes already described. The best photocurrent output is obtained upon illumination through glass (curve 1b). In the diffusion-limited region the magnitude of the photocurrent corresponds well to the measured monochromatic quantum yield. When comparing this system with that based on zinc oxide ceramic electrodes [see Fig. 3(*b*)] a striking difference in the photocurrent output is evident. Its magnitude is a factor of *ca.* 1.8 (at 0.4 V *vs.* NHE) lower than the photocurrent obtained from the titanium dioxide film with frontal illumination. After dipping similar films for longer periods of time (*ca.* 130 h) in a 5 × 10^{-3} mol dm^{-3} solution of the copper complex, in another set of experiments, the photocurrent measured, under the same conditions, was enhanced as shown in Fig. 3(*a*) (*cf.* curves 1b and 2b). This shows that a longer residence time favours the adsorption of the copper(I) complex onto the surface film, thus stressing the advantage of using semiconducting films based on colloidal particles due to the enhancement of the surface geometry projection of these systems. The cathodic peak at *ca.* −0.1 V is due to some impurities on the substrate [*cf.* curves 2 in Fig. 3(*a*)]. In both systems, under monochromatic illumination, the photopotential (within experimental error) is the same, *i.e.* $V_{ph} \approx 0.3$ V. The relative energies of the corresponding species at the semiconducting electrode interface are depicted in Fig. 4.

The position of the conduction band edge, E_c, of titanium dioxide films (E_g = 3.2 eV, anatase) is located at *ca.* −0.65 V *vs.* NHE. Under the same conditions, the energy conduction band of zinc oxide material (E_g = 3.2 eV) is at *ca.* −0.28 V *vs.* NHE.[25] The Fermi level in both systems was 0.1 V below the conduction band, and $E_{\frac{1}{2}}$ (hydroquinone–quinone) = 0.34 V *vs.* NHE (pH 6.5). According to Fig. 4, a maximum photopotential, V_{ph} (difference between the Fermi level of the conduction band electrons and the redox potential of the electron donors), of *ca.* 0.5 V is expected for the zinc oxide system, and 0.88 (pure anatase)–0.68 V (pure rutile) for the titanium dioxide film. The

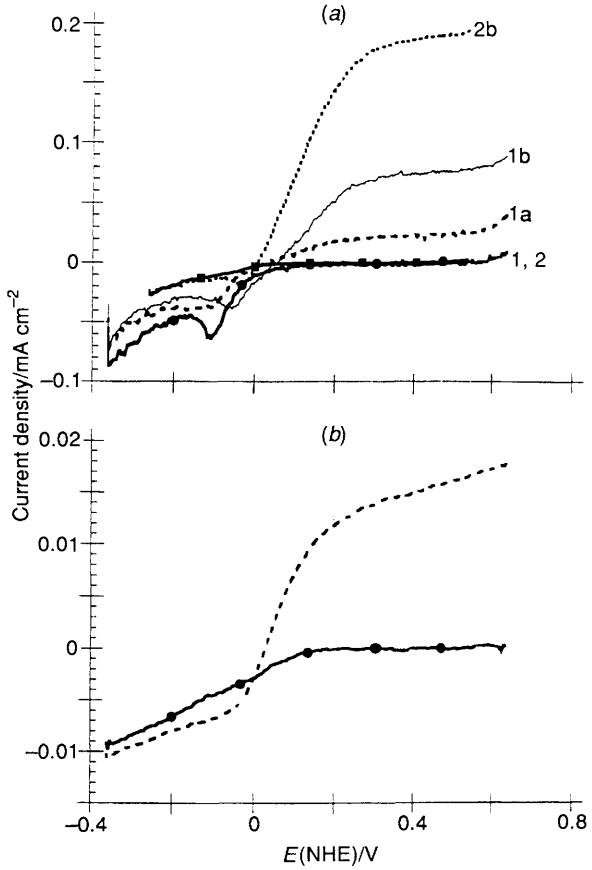

Fig. 3 Potentiostatic photocurrent *vs.* potential characteristics of (*a*) titanium dioxide films sensitized with the copper(I) complex in 0.4 mol dm^{-3} Na_2SO_4 + 5 × 10^{-3} mol dm^{-3} hydroquinone (curves: 1 and 2, in darkness; 1a, frontal illumination; 1b and 2b, rear illumination) and (*b*) the zinc oxide ceramic sensitized system [in darkness (——) and with illumination (- - -)]. In both cases the illumination was provided by a band-pass filter (500 nm), intensity *ca.* 50 mW cm^{-2}

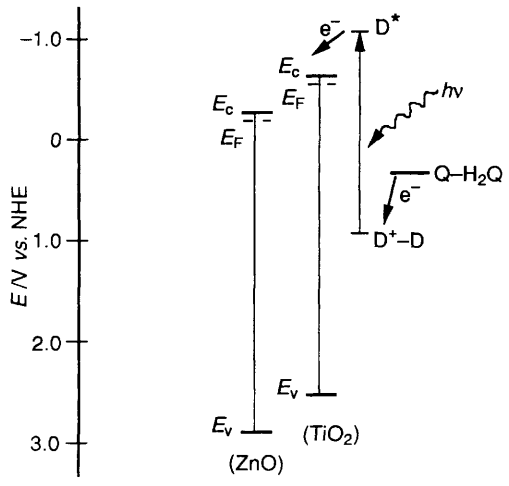

Fig. 4 Energy levels (conduction bands, E_c; valence bands, E_v; and Fermi level, E_F) of zinc oxide and titanium dioxide films (pH 6.5). The redox potentials of the adsorbed dye, D = $[CuL_2]^+$ **1**, and quinone (Q)–hydroquinone (H_2Q) are also indicated

powder employed for the fabrication of films was a mixture of 30% rutile and 70% anatase. Under monochromatic illumination (using a 500 nm band-pass filter) the current–potential characteristics, under similar conditions, were more favourable in the titanium dioxide systems, *cf.* Figs. 2 and 3. Therefore, a preliminary study of the photoelectrochemical cell in a regenerative mode based on such films was tested.

Regenerative Photoelectrochemical Cell.—Since the regeneration of the photooxidized dye occurs more rapidly when using iodide than hydroquinone in the electrolyte, we performed measurements in a non-aqueous electrolyte solution, 0.14 mol dm^{-3} KI + 16 × 10^{-3} mol dm^{-3} I_2 in propylene carbonate, in a single-compartment three-electrode cell. A carbon rod and platinum were used as the counter and reference electrodes, respectively. Potentiostatic measurements were performed on two coated titanium dioxide films which were previously tested in an aqueous electrolyte. Fig. 5(*a*) contrasts these results.

The photocharacteristic (fill factor, f.f.) is a function of the quality of the films as deduced from the form of the current *vs.* potential curves 1 and 2 in darkness and upon illumination. Using a cut-off filter (G475), similar photocurrent densities are obtained in the saturation region for both electrodes (1b and 2b). The photocurrent saturation of sample 2 extends to *ca.* 0.4 V decreasing to a maximum photopotential of 0.6 V as predicted above. For sample 1 the maximum photopotential reached was 0.5 V. According to Fig. 4, we must assume that, in the non-aqueous environment, the flat-band region for titanium dioxide films is located between 0.68 and 0.88 V above the redox potential of I^-–I_3^-. The onset of the dark current at a potential more positive than that of the flat band (as in the case of sample 1) indicates that the reduction of I_3^- is effected by the conduction band electrons, n_{cb}, acting as recombination centres upon illumination, thus reducing the photopotential according to the simple diode equation $V_{ph} = (kT/e) \ln (j_{ph}/j_d)$,[30] where j_{ph} = sensitized photocurrent, the dark current $j_d = n_{cb}k[I_3^-]$ according to ref. 31 and e is the elementary charge. After several hours of continuous working, with the cut-off filter (G475), the photocurrent (curve 1b) of sample 1 decreased to the level of the curve recorded with a band-pass filter (curve 1a) but the photopotential was maintained (0.5 V). This effect may be due to desorption or possible labilization of the copper complex. Using a solar-cell arrangement (two electrodes in the same electrochemical cell) with varying resistances, we recorded the photocharacterstic of the titanium dioxide film (sample 2), *cf.* Fig. 5(*a*). The photocurrent *vs.* potential is shown in Fig. 5(*b*). The shape of the curve fully matches that recorded in the

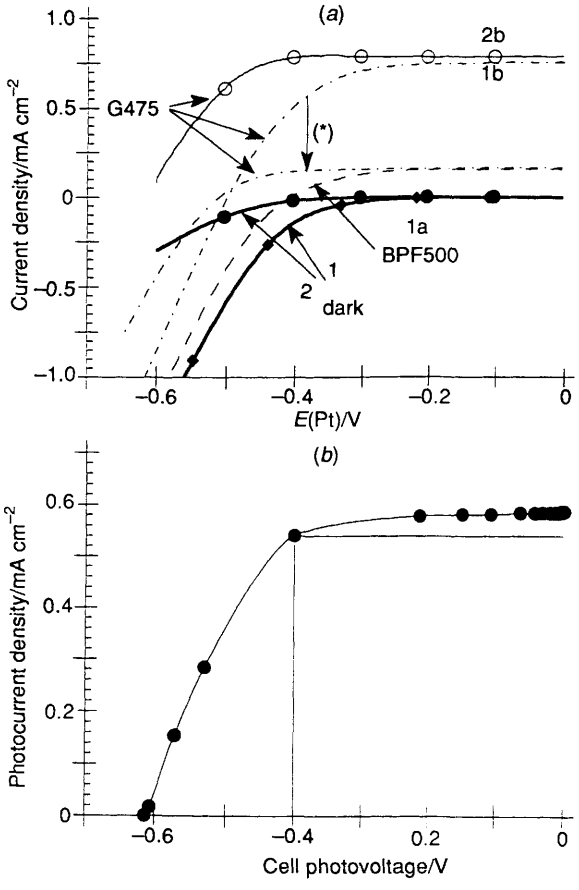

Fig. 5 (*a*) Potentiostatic current *vs.* potential characteristics of two titanium dioxide films recorded in 0.14 mol dm^{-3} KI + 16 × 10^{-3} mol dm^{-3} I_2 in propylene carbonate in darkness (1,2). Curve 1a was recorded with a band-pass filter (BFP500, 500 nm, ≈50 mW cm^{-2}), 1b and 2b with a cut-off filter (G475, ≈300 mW cm^{-2}); curve 1b decreases with time to the level of curve 1a, indicated by the arrow (*). (*b*) Photocurrent *vs.* voltage characteristics (solar arrangement) for the case 2b in (*a*)

potentiostatic mode. The factor f.f. (=maximum output power/short circuit current × photovoltage) is 0.60. The maximum output power is represented by the rectangle under the curve. The conversion efficiency is still low, but measurements performed under the same conditions, with the ruthenium complex reported by O'Regan and Grätzel,[12] showed that the photocurrent saturation is a factor of 3 higher than in our system. The same tendency of the photocurrent to decrease was also observed.

A crucial factor for the development of solar cells based on sensitization *via* transition-metal complexes is long-term stability. In the present system a degradation with time was observed, *i.e.* the photocurrent decreased whereas the photopotential was maintained. Although a higher kinetic stability is expected for the copper(I) in comparison to the ruthenium(II) complex, we are still unable to give a plausible explanation for the photocurrent decrease. The band enhancement at *ca.* 600 nm, observed with the hydroquinone-containing electrolyte, might represent an advantage from the point of view of a better harvesting of the visible light absorption at lower energies if a means is found to stabilize such an interface under working conditions. Furthermore, the comparison between ZnO (ceramic) and TiO_2 (films) shows that derivatization *via* carboxylate ligands is not the only precondition to facilitate the charge transfer. The oxidation state of the metal centre in an oxide matrix (Zn^{2+} in ZnO; Ti^{3+}, Ti^{4+} in TiO_2) appears to play an important role at the interface (as qualitatively shown by FTIR measurements). Thus it may

favour co-ordination effects, that is, a dynamic change in the co-ordination sphere of the complex. The effect of the thin-layer thickness on the photocurrent action spectra of $[RuL_2(NCS)_2]$ reported by Nazeeruddin *et al.*[14] may be related to the modification of the co-ordination sphere probably induced by the increasing number of defects (Ti^{3+}-like?) with increasing porosity of the matrix on the titanium dioxide films. Infrared or Raman measurements *in situ* are necessary to assess the origin of this phenomenon.

Conclusion

The present study has identified a new class of heterogeneous sensitizers for photoelectrochemical cells based on titanium dioxide colloidal films and a copper(I) complex of carboxylate-substituted 1,10-phenanthroline. Sensitization of zinc oxide ceramic electrodes under the same conditions demonstrated the role of the structured surface gained with colloidal particles. With the copper(I) complex one might attain a photopotential of *ca.* 0.6 V. No effort was made to optimize such a system due to the difficulty in sustaining the sensitized photocurrent as a function of time. Further, the photocurrent action spectrum measured in a hydroquinone-containing electrolyte is enhanced at lower absorption energies. This might represent an advantage for light-energy conversion on oxide semiconductor devices based on a copper(I) complex which covers almost the whole visible solar spectral region.

Acknowledgements

We thank the French Ministry of Research and Technology for a fellowship (to J.-F. N.), Dr. C. O. Dietrich-Buchecker for helpful discussions, Mr. G. Smestad for his advice in the preparation of titanium dioxide colloidal electrodes as well as his stimulus to undertake this work and Mr. D. Jockisch and Mr. C. Ureche for their technical assistance in the preparation of films. Thanks are also due to Mr. R. Grünwald for his help with the FTIR measurements. This work was in part supported by a grant from the Bundes Ministerium für forschung und Technologie.

References

1 A. J. Bard, H. D. Abruña, C. E. Chidsey, L. R. Faulkner, S. W. Feldberg, K. Itaya, M. Majda, O. Melroy, R. W. Murray, M. D. Porter, M. P. Soriaga and H. S. White, *J. Phys. Chem.*, 1993, **97**, 7147.
2 N. Alonso-Vante and H. Tributsch, in *Electrochemistry of Novel Materials*, eds. J. Lipkowski and Ph. Ross, VCH, 1994, vol. 3, p. 1.
3 H. Tributsch, Thesis dissertation, Technical University, Munich, 1968.
4 R. Memming and H. Tributsch, *J. Phys. Chem.*, 1971, **75**, 562.
5 M. Nakao, K. Itoh and T. Watanabe, *Ber. Bunsenges. Phys. Chem.*, 1985, **89**, 134.
6 E. Daltrozzo and H. Tributsch, *Photogr. Sci. Eng.*, 1975, **19**, 308.
7 T. Watanabe, T. Takizawa and K. Honda, *Ber. Bunsenges. Phys. Chem.*, 1981, **85**, 430.
8 L. Bahadur and J. P. Pandey, *J. Appl. Electrochem.*, 1993, **22**, 883.
9 L. K. Chau, C. Arbour, G. E. Collins, K. W. Nebesny, P. A. Lee, C. D. England, N. R. Armstrong and B. A. Parkinson, *J. Phys. Chem.*, 1993, **97**, 2690.
10 A. Kay and M. Grätzel, *J. Phys. Chem.*, 1993, **97**, 6272.
11 R. Amadelli, R. Argazzi, C. A. Bignozzi and F. Scandola, *J. Am. Chem. Soc.*, 1990, **112**, 7099.
12 B. O'Regan and M. Grätzel, *Nature (London)*, 1991, **353**, 373.
13 O. Enea, J. Moser and M. Grätzel, *J. Electroanal. Chem. Interfacial Electrochem.*, 1989, **259**, 59.
14 M. K. Nazeeruddin, A. Kay, I. Rodicio, R. Humphry-Baker, E. Müller, P. Liska, N. Vlachopoulos and M. Grätzel, *J. Am. Chem. Soc.*, 1993, **115**, 6382.
15 C. O. Dietrich-Buchecker, P. A. Marnot, J.-P. Sauvage, J. P. Kintzinger and P. Maltèse, *New. J. Chem.*, 1984, **8**, 573.
16 C. O. Dietrich-Buchecker, P. A. Marnot and J.-P. Sauvage, *Tetrahedron Lett.*, 1982, **23**, 5291.
17 N. Alonso-Vante, V. Ern, P. Chartier, C. O. Dietrich-Buchecker, D. R. McMillin, P. A. Marnot and J.-P. Sauvage, *Nouv. J. Chim.*, 1983, **7**, 3.
18 C. O. Dietrich-Buchecker and J.-P. Sauvage, *Tetrahedron*, 1990, **46**, 503.
19 R. A. Leising, J. J. Grzybowski and K. J. Takeuchi, *Inorg. Chem.*, 1988, **27**, 1020.
20 H. Gilman and J. Swiss, *J. Am. Chem. Soc.*, 1940, **62**, 1847.
21 S. Chardon-Noblat and J.-P. Sauvage, *Tetrahedron*, 1991, **47**, 5123.
22 R. G. Curtis, S. I. Heilbron, E. R. H. Jones and G. F. Woods, *J. Chem. Soc.*, 1953, 457.
23 N. Alonso-Vante, M. Beley, P. Chartier and V. Ern, *Rev. Phys. Appl.*, 1981, **16**, 5.
24 C. O. Dietrich-Buchecker, P. A. Marnot, J.-P. Sauvage, J. R. Kirchhof and D. R. McMillin, *J. Chem. Soc., Chem. Commun.*, 1983, 5291; 1984, 204.
25 N. Alonso-Vante, Thesis dissertation, Université Louis Pasteur, Strasbourg, 1984.
26 A. Hagfeldt, U. Björksten and S.-E. Lindquist, *Sol. Energy Mat. Sol. Cells*, 1992, **27**, 293.
27 O. Poizat and C. Sourisseau, *J. Phys. Chem.*, 1984, **88**, 3007.
28 N. Alonso-Vante, unpublished work.
29 A. El Hajbi, N. Alonso-Vante, P. Chartier, G. Goetz-Grandmont, R. Heimburger and M. J. F. Leroy, *J. Electroanal. Chem. Interfacial Electrochem.*, 1986, **207**, 127.
30 R. Memming, in *Photochemistry and Photophysics*, ed. J. F. Rabeck, CRC Press, Boca Raton, FL, 1990, vol. 2, p. 143.
31 A. Kumer, P. G. Santangelo and N. S. Lewis, *J. Phys. Chem.*, 1992, **96**, 835.

Received 18*th January* 1994; *Paper* 4/00313F